

EFFECT OF THE CUBIC NONLINEARITY AND MULTIPHOTON IONIZATION ON SPATIOTEMPORAL BEHAVIOR OF A SUBPICOSECOND LASER PULSE IN AIR

V.P. Kandidov, O.G. Kosareva, and S.A. Shlenov

*M.V. Lomonosov State University, Moscow
Received September 14, 1992*

Transformation of a laser pulse frequency spectrum and spatiotemporal distribution of radiation over the waist of a beam focused into air are numerically investigated. The effects of the Kerr nonlinearity and plasma nonlinearity due to multiphoton ionization of neutral molecules are considered. It is shown that both symmetric and blue asymmetric broadening of the transmitted pulse spectrum can be observed depending on the degree of beam focusing.

Propagation of high-power subpicosecond laser pulses in air is accompanied by transformation of their frequency spectrum at distances of several meters.¹ For focused beams this transformation occurs in the beam waist. The case in point is the pulses of ~ 100 fs duration with power of the order of 10^9 W and $\sim 10^9$ – 10^{15} W/cm² intensity in the beam waist.

In the experiments the authors of Ref. 2 observed large broadening of the spectrum which resembles the phase self-modulation (PSM) arising from cubic nonlinearity. Substantially different character of spectrum transformation under similar experimental conditions was reported in Ref. 3. When the beam was focused into air, the spectrum shifted toward the blue region without detectable broadening. The authors believed that the blue shift of the spectrum was engendered by free charge carriers generated due to multiphoton ionization of molecules in the beam waist.

Various possible mechanisms of spectrum transformation are discussed in the literature.^{1,4} The important factor is that the nonlinearity engendering the spectrum transformation must be sufficiently fast to provide variation of the optical properties of the medium on subpicosecond scale. For subpicosecond pulses at least two mechanisms of nonlinearity may result in qualitatively different transformations of the frequency spectrum.

In this paper we examine the general behavior of spatiotemporal (including spectral) characteristics of the subpicosecond pulse during its focusing into air with allowance for the joint effect of cubic nonlinearity and free-electron generation self-consistent with the field.

In the study of the pulses of subpicosecond duration, the variation in the refractive index of air is determined by nonlinear effects whose relaxation time τ_{nl} does not exceed 10^{-13} s. Among these are the electron and orientational Kerr effects and nonlinear ionization.^{5,6,7} If the contribution of these effects is assumed to be additive, the total perturbation of the refractive index δn can be written down as

$$\delta n = \Delta n_e + \Delta n_{or} + \Delta n_p. \quad (1)$$

For electron nonlinearity Δn_e associated with redistribution of electron density over isotropic molecules

the characteristic time is $\tau_{nl} \approx 10^{-15}$ s provided that the radiation frequency is off the absorption band. In this case

$$\Delta n_e = \frac{1}{2} n_{2e} |E|^2. \quad (2)$$

Under normal conditions the nonlinearity coefficient for air is $n_{2e} \approx 10^{-16}$ cm³/erg (see Ref. 8).

The characteristic time τ_{nl} of orientational effect is of the order of 10^{-13} – 10^{-12} s, and relaxation of the refractive index perturbation is described by the relaxation equation

$$\left(\tau_{nl} \frac{\partial}{\partial t} + 1 \right) \Delta n_{or} = \frac{1}{2} n_{2or} |E|^2, \quad (3)$$

where $n_{2or} \approx n_{2e}$ (see Ref. 8).

Ionization of the gas in a strong light field results in the formation of free charges that leads to variations in optical properties of the medium. For radiation of subpicosecond duration, probability of collision of the formed electrons with molecules of gaseous components is small, and the collisional (electron) ionization can be neglected. Radiation-induced plasma is weakly ionized; by the time of pulse termination the degree of ionization attains the value of the order of 10^{-2} – 10^{-1} . In this case the plasma frequency is $\omega_p \approx 10^{13}$ s⁻¹, and the medium remains optically transparent for visible radiation. Within the time over which the subpicosecond pulse acts there is no optical breakdown by commonly accepted definition which is associated with radiation blocking, light burst, and harsh sound.

If the energy of the free electrons in the process of multiphoton ionization is assumed to be of the order of 1–10 eV, then the Debye radius of the originating plasma $r_D \approx 10^{-8}$ m. In this case even for strong focusing of a beam the condition of spatial quasineutrality $r_D \ll l$ holds for plasma, where l is the spatial scale of plasma formation. Moreover, the approximation of an ideal plasma is valid for which the number of particles inside the Debye sphere is large

$$\frac{4}{3} \pi r_D^3 N_0 \gg 1, \quad (4)$$

where N_0 is the concentration of neutral molecules in air. Thus for plasma generated by the subpicosecond pulse we

may introduce the macroscopic parameters specifying its optical properties.

The contribution of a plasma component to variation in the index of refraction is

$$\Delta n_p = -\omega_p^2 / 2 \omega^2, \quad (5)$$

where $\omega_p^2 = 4\pi e^2 N_e / m$. Here ω is the radiation frequency, e and m are the charge and mass of an electron. Since within the time over which the subpicosecond laser pulse acts the avalanche processes have no time to develop, multiphoton or tunnel ionization of air–mixture components can serve as a source of free electrons. In this case, based on the values of the adiabatic exponent γ (see Ref. 5), for laser pulses with intensities $I \leq 10^{14}$ W/cm² the first, i.e., multiphoton mechanism of ionization is most probable in the visible spectral range. Let the time of electron–ion recombination be greater than the pulse duration. Then, since the energy of the most part of the free electrons does not exceed 10 eV, they have no time to leave the beam waist (its transverse size is of the order of 1 μ m) and remain at points of their origin. In this case the concentration of the free electrons N_e is determined by the rate of multiphoton ionization at the same point in space and monotonically increases with time

$$N_e(r, t) = \int_{t_0}^t \frac{dN_e}{dt} dt, \quad N_e(r, t_0) = 0. \quad (6)$$

The rate of multiphoton ionization, in its turn, depends on radiation intensity.

Thus the contribution of plasma component to the index of refraction is local in space and is given by formulas (3) and (4).

To determine the ionization rate, we make use of a simple model⁷ in which the quantum–mechanical calculation of dN_e/dt is made for a hydrogen–like atom on the assumption that in the presence of the variable electromagnetic field only the wave function of a free electron varies. In spite of a simplified form of the model in which the medium enters only through the ionization potential, it describes sufficiently well the experiments on multiphoton ionization of gases.⁹ Such a model was successfully employed in the comparative analysis of the experimental data¹⁰ on the transformation of frequency spectrum in xenon and the numerical calculations.¹¹

In air the principal contribution to generation of the free electrons in the process of multiphoton ionization comes from the components with the highest partial pressure, i.e., nitrogen and oxygen. The contribution of the rest of the components is negligible.

The dynamics of the free electron formation upon exposure to a rectangular pulse of duration $\tau = 1$ ns at the wavelength $\lambda = 308$ nm with intensity $I = 10^{14}$ W/cm² is depicted in Fig. 1. During the first approximately 350 fs the most part of the free electrons is represented by the oxygen electrons since the ionization potential of oxygen is smaller than that of nitrogen. During this time oxygen is almost completely ionized and the subsequent "growth" of the free carriers of charge is provided by nitrogen molecules since their concentration remains sufficiently high even 1 ps later. We hereafter ignore the effects of multiple ionization because the ionization potential of gaseous components of air is much higher and the rate of ionization is correspondingly lower than those of nitrogen molecules.

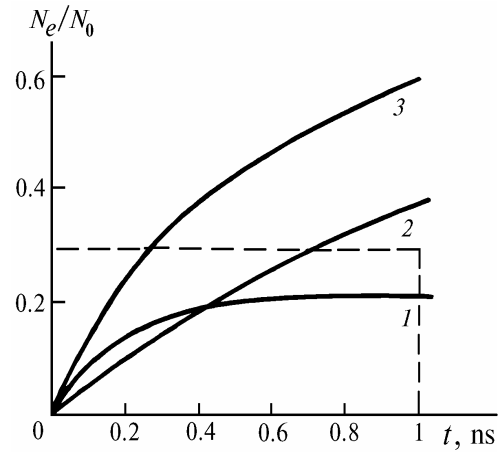


FIG. 1. Variation of the concentration of free carriers of charge within the time over which the rectangular pulse with the intensity $I_0 = 10^{14}$ W/cm² acts (dashed line); 1) oxygen electrons, 2) nitrogen electrons, and 3) total concentration of oxygen and nitrogen electrons; N_0 is the initial concentration of neutral molecules.

Since the really high intensities of radiation are obtained in strongly focused beams, the model of radiation propagation incorporates the beam passage through the beam waist region, where both nonlinear and diffraction effects are primarily manifested. To this end we use the parabolic diffraction equation for a complex amplitude of the electric field E :

$$2i\kappa \left(\frac{\partial}{\partial z} + \frac{1}{v_g} \frac{\partial}{\partial t} \right) E = \Delta_{\perp} E + 2\kappa^2 \frac{dn}{n_0} E - i\kappa\alpha_{nl} [I] E. \quad (7)$$

Here z is the direction of beam propagation, v_g is the group velocity, Δ_{\perp} is the transverse Laplacian, and δn is the nonlinear increment to the refractive index given by Eq. (1). We assume here that the value of n_2 remains unchanged in the process of ionization of neutral molecules. The last term in Eq. (7) describes nonlinear losses of radiation due to multiphoton ionization.

We ignored the variance of the group velocity in Eq. (7). In fact, on the assumption that the radiation at the wavelength λ is far from resonances of molecular atmospheric constituents, the dispersion length of the subpicosecond pulse amounts to hundreds of meters. The dispersion length in the pulse–induced plasma in the case of complete ionization of neutral molecules decreases down to 1 m. However, the size of the beam waist in which the degree of ionization is high does not exceed 1 mm.

In the numerical experiments the propagation of axially symmetric focused beams with Gaussian profile were considered in the case of emission of Gaussian pulse with band–limited spectrum

$$E(z = 0, \rho, t) = E_0 \exp\left(-\frac{t^2}{2\tau_0^2}\right) \exp\left(-\frac{\rho^2}{2a_0^2} + i\frac{\kappa\rho^2}{2R_f}\right). \quad (8)$$

In the calculations we considered a wide range of the parameters of radiation at the wavelengths $\lambda = 308$ and 628 nm whose duration τ_0 varied from 85 to 350 fs. The peak radiation power was chosen close in value to critical power of self–focusing which was $3.3 \cdot 10^8$ W for $n_2 = 10^{-16}$ cm³/erg (see Ref. 8) at $\lambda = 308$ nm. For the beam diameter

$a_0 = 0.3$ cm the peak intensity at the output aperture was taken $I_0 = 9.4 \cdot 10^8$ W/cm². Such a value of the intensity was insufficient for the effective multiphoton ionization, and in the pulse spectrum upon exiting the beam waist we observed symmetric broadening typical of the PSM. The structure of the broadened spectrum remained unchanged due to spatial self-compression of the beam¹² at least for moderate parameters of nonlinearity.¹³

However, the situation changes for focused beams of the same power. Depicted in Fig. 2 are the frequency spectra calculated for radiation on the beam axis after its passage through the beam waist region. The parameter of the curves is the beam focusing radius. It can be seen that in the case of weak focusing (curve 1) the frequency spectrum differs slightly from the symmetric one; its broadening and modulation structure are determined by the electron component of the Kerr nonlinearity. Some asymmetry in the spectrum is accounted for by contribution of multiphoton ionization. As the analysis shows, the orientational nonlinearity does not in fact influence the pulse spectrum.

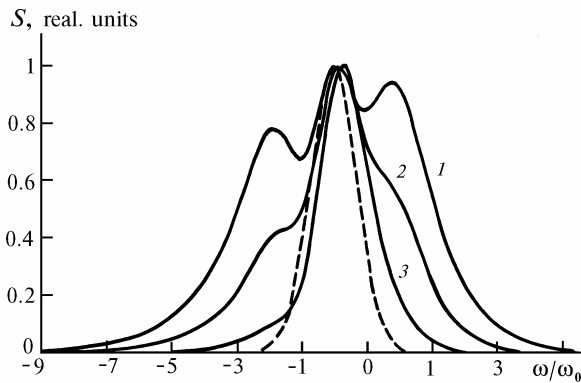


FIG. 2. Spectral density of radiation power on the axis of the focused beam. 1) $R_f = 110$, 2) $R_f = 80$, and 3) $R_f = 40$ cm. Dashed curve denotes the input pulse spectrum. Here ω_0 is the width of the input pulse spectrum at a level e^{-1} , $I_0 = 9.4 \cdot 10^8$ W/cm², and $a_0 = 0.3$ cm.

For stronger focusing the intensity in the beam waist increases and in the region near the focus the free-electron concentration becomes larger. The number of these electrons increases with time, a linear trend appears in phase modulation of the pulse, and the position of the center of gravity of the frequency spectrum shifts toward the region of higher frequencies (curve 2). In this case as the radius of focusing becomes smaller and, correspondingly, the contribution of ionization nonlinearity increases, the modulation structure of the spectrum vanishes in the anti-Stokes region and substantially decreases in the Stokes one (curve 3). Thus the ionization nonlinearity seems to suppress the Kerr one.

With low, compared to critical, beam power under conditions of strong focusing it is possible to attain high intensity at which the contribution of the Kerr nonlinearity is negligible, and the spectrum transformation is determined by multiphoton ionization. In this case the spectrum shift of the Gaussian pulse toward a blue region is accompanied by its broadening which is characterized by stretching of the Stokes wing and is due to the nonlinear temporal dependence of the pulse phase. Two factors are responsible for frequency

change: a nonrectangular pulse shape and depletion of a source of free carriers, i.e., neutral molecules, by the time of the pulse termination (see Fig. 1) which slows down the frequency growth. As a result, the pulse frequency modulation becomes of complicated nature and the shape of the shifted spectrum differs from the Gaussian one.

In the experiments a frequency spectrum is recorded, as a rule, on the entire beam aperture. Figure 3 depicts the aperture-averaged pulse spectrum. This spectrum has no principal difference from the spectrum on the beam axis, it is shifted toward a blue region by the value $0.2 \omega/\omega_0$ measured from the position of the center of gravity of the spectral distribution. It should also be noted that smoothing of the modulation structure in the average spectrum is less pronounced than that in the spectrum on the beam axis.

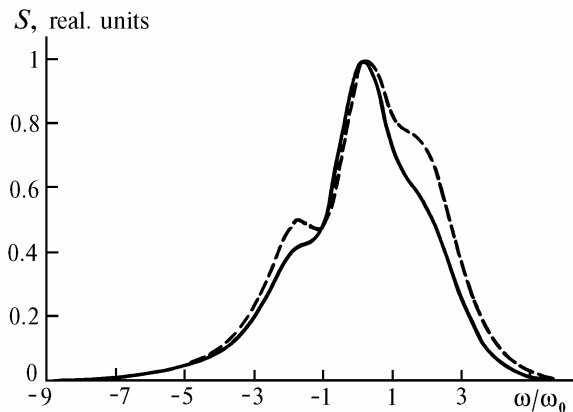


FIG. 3. Spectral power density on the beam axis and aperture-averaged one (dashed curve) for $R_f = 80$ cm, $I_0 = 9.4 \cdot 10^8$ W/cm², and $a_0 = 0.3$ cm.

Formation of free electrons in the high-intensity region, i.e., first of all on the beam axis, gives rise, following Eq. (5), to the formation of a defocusing "lens" whose optical strength increases with time. Therefore, the radiation is expelled from the near-axis region. Depicted in Fig. 4 is the spatial intensity distribution over the beam waist obtained at different instants of time. It can be seen in what way the Gaussian beam shape suffers distortions in the edge of the pulse. Upon entering the beam waist the effect of ionization on the transverse profile shape is insignificant and is manifested only by the instant of time $t = \tau_0$ (Fig. 4a): the near-axis part of the beam becomes plane. In the beam waist the number of free carriers increases faster with time. Ionization defocusing becomes pronounced by the time $t = 0.3\tau_0$. The intensity on the beam axis becomes lower than that in the periphery (Fig. 4b) and the beam acquires a distinctly pronounced annular structure. In this case the peak intensity diminishes down to $1.7 \cdot 10^{14}$ W/cm² in contrast to its value of $2 \cdot 10^{14}$ W/cm² in the linear beam waist and is attained on the beam axis at time $t = -0.3\tau_0$ (in the running system of coordinates).

It should be noted that a dip on the beam axis is not related to the loss of energy due to generation of the carriers since the losses remain also insignificant in the case shown in Fig. 4 and do not exceed 4% of the initial pulse energy. After propagation through the nonlinear focus the dip on the axis disappears due to beam diffraction (Fig. 4b).

The transverse profile transformation in the far diffraction zone within the time over which the pulse acts

can be traced by examining the angular spectrum shape upon exiting the beam waist (Fig. 5). In the pulse edge the angular spectrum possesses a Gaussian shape and in fact coincides with the input beam spectrum (Fig. 5a). In

the course of time the angular spectrum shape transforms: at $t = 0$ a local minimum is formed for $\kappa = 0$ (Fig. 5b) and by $t = \tau_0$ a near-axis section of the spectrum is flattened (Fig. 5c).

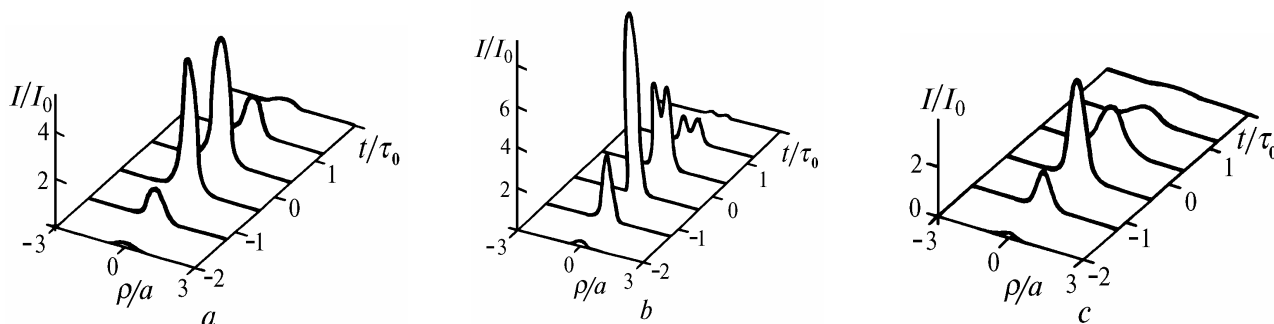


FIG. 4. Variation in the intensity transverse distribution in different planes z within the time over which the pulse acts: $z = -1$ (a), 0 (b), and 1 (c). $I_0 = 2 \cdot 10^{13}$ W/cm², the coordinate z is normalized to the confocal parameter of the beam and is counted off from the beam waist in the linear medium, and a is the beam radius in the plane $z = -3$.

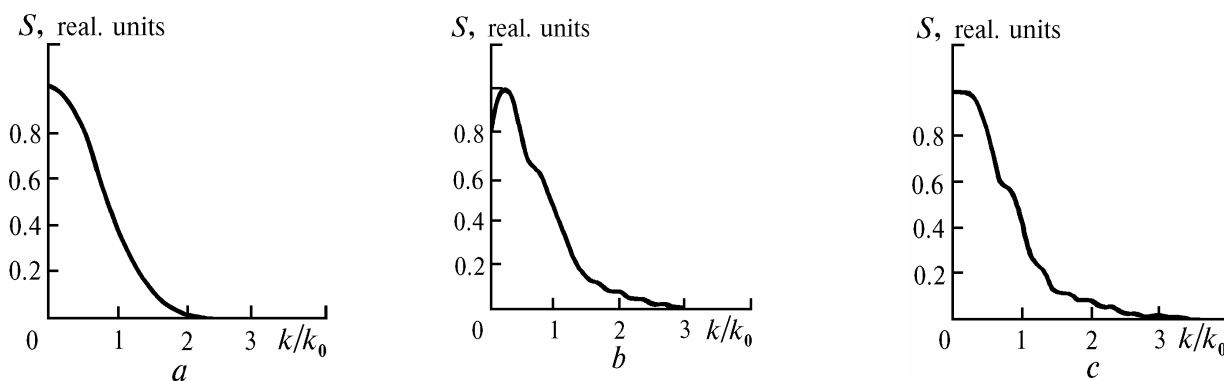


FIG. 5. Angular beam spectrum at different instants of time t : $t = -\tau_0$ (a), 0 (b), and τ_0 (c). Here k_0 is the angular beam spectrum halfwidth upon entering the nonlinear medium.

The beam profile in the far diffraction zone also behaves correspondingly. The comprehensive analysis shows that deformation of the transverse beam profile in the far diffraction zone is primarily due to the deviation of the transverse intensity distribution from the Gaussian one upon exiting the beam waist.

Thus when a high-power subpicosecond pulse propagates in air, the self-action phenomenon can appear due to the Kerr nonlinearity and multiphoton ionization. These two mechanisms of nonlinearity make a competitive impact on the transformation of the frequency spectrum and spatial distribution of radiation. The choice of radiation parameters, in particular focusing radius, can weaken the effect of the Kerr nonlinearity and, correspondingly, transform the pulse frequency spectrum after beam focusing.

REFERENCES

1. S.A. Akhmanov, V.A. Vysloukh, and A.S. Chirkin, *Optics of Femtosecond Laser Pulses* (Nauka, Moscow, 1988).
2. D. Kuhlke, U. Herpers, and D. von der Linde, *Opt. Comm.* **63**, 275 (1987).
3. W.M. Wood, G. Focht, and M.C. Downer, *Opt. Lett.* **13**, 984 (1988).
4. P.B. Corkum and C. Rolland, *IEEE J. Quantum Electron.* **25**, 863 (1989).
5. N.B. Delone and V.P. Krainov, *Atom in a Strong Light Field* (Energoizdat, Moscow, 1984), 224 pp.
6. V.E. Zuev, A.A. Zemlyanov, and Yu.D. Kopytin, *Nonlinear Optics of the Atmosphere* (Gidrometeoizdat, Leningrad, 1989), 256 pp.
7. A. Szoke, *NATO ASI Series Physics B* **171**, 207 (1988).
8. Y. Shimoji, *J. Opt. Soc. Am.* **B 6**, 1994 (1989).
9. M.D. Perry, O.L. Landen, and A. Szoke, *Phys. Rev. A* **37**, 747 (1987); *Phys. Rev. Lett.* **60**, 1720 (1988).
10. P.B. Corkum and C. Rolland, *NATO ASI Series Physics B* **171**, 157 (1988).
11. O.G. Kosareva and S.A. Shlenov, *Izv. Akad. Nauk SSSR, Ser. Fiz.* **56**, No. 9, 56–62 (1992).
12. S.A. Shlenov, *Izv. Akad. Nauk SSSR, Ser. Fiz.* **55**, No. 2, 363 (1991).
13. A.M. Kochetkova and S.A. Shlenov, *Atm. Oceanic Opt.* **5**, No. 2, 99–102 (1992).